Environmental Science & Technology

pubs.acs.org/est

Article

SARS-CoV-2 RNA in Wastewater Settled Solids Is Associated with COVID-19 Cases in a Large Urban Sewershed

Katherine E. Graham, Stephanie K. Loeb, Marlene K. Wolfe, David Catoe, Nasa Sinnott-Armstrong, Sooyeol Kim, Kevan M. Yamahara, Lauren M. Sassoubre, Lorelay M. Mendoza Grijalva, Laura Roldan-Hernandez, Kathryn Langenfeld, Krista R. Wigginton,* and Alexandria B. Boehm*

Cite This: *Environ. Sci. Technol.* 2021, 55, 488−498

Read Online

ACCESS | Metrics & More | Article Recommendations | Supporting Information

ABSTRACT: Wastewater-based epidemiology may be useful for informing public health response to viral diseases like COVID-19 caused by SARS-CoV-2. We quantified SARS-CoV-2 RNA in wastewater influent and primary settled solids in two wastewater treatment plants to inform the preanalytical and analytical approaches and to assess whether influent or solids harbored more viral targets. The primary settled solids samples resulted in higher SARS-CoV-2 detection frequencies than the corresponding influent samples. Likewise, SARS-CoV-2 RNA was more readily detected in solids using one-step digital droplet (dd)RT-PCR than with two-step RT-QPCR and two-step ddRT-PCR, likely owing to reduced inhibition with the one-step ddRT-PCR assay. We subsequently analyzed a longitudinal time series of 89 settled solids samples from a single plant for SARS-CoV-2 RNA as well as coronavirus recovery (bovine coronavirus) and fecal strength (pepper mild mottle virus) controls. SARS-CoV-2 RNA targets N1 and N2 concentrations correlated positively and significantly with COVID-19 clinically confirmed case counts in the sewershed. Together, the results demonstrate that measuring SARS-CoV-2 RNA concentrations in settled solids may be a more sensitive approach than measuring SARS-CoV-2 in influent.

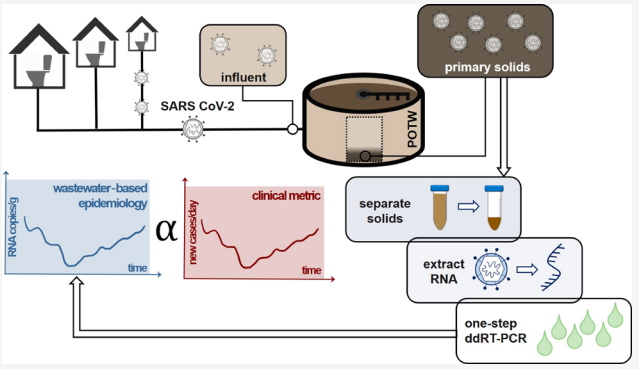

INTRODUCTION

Municipal wastewater is a composite biological sample of an entire community with each member of the community inputting biological specimens every day. It is therefore no surprise that wastewater has been tapped as an epidemiological tool to gauge aspects of public health, such as narcotic usage,[1,2] the reemergence of poliovirus,[3,4] and infection rates of viral[5,6] and bacterial[7,8] diseases. COVID-19 has accelerated the interest in wastewater-based epidemiology (WBE) due to the fact that SARS-CoV-2 genes are detected in the feces of many infected individuals.[9−11] More established epidemiological tools used to track cases in a community have been hindered during the COVID-19 pandemic by diagnostic kit shortages,[12] asymptomatic or mild cases that do not encounter the medical system or delay seeking medical attention,[13] and the lag times between testing and reporting.[14] As a result, public health officials and administrators have had to make critical decisions about opening or closing communities with limited surveillance data. Scientists, engineers, public officials, and the general public, are optimistic that WBE could provide additional data on COVID-19 infections in a community. In fact, the United States Center for Disease Control has established the National Wastewater Surveillance System as a framework for using WBE to inform the response to the COVID-19 pandemic.[15]

Recent published studies have reported SARS-CoV-2 detection and quantification in sewage.[16−18] Based on these reports, numerous entities/organizations across the globe and across scales are moving to implement WBE. It remains to be seen how the data generated from wastewater surveillance should be interpreted or will ultimately be used to make public health decisions. Potential uses include informing on the presence or absence of COVID-19 in a community, similar to polio surveillance;[4] tracking trends over time to project infection trajectory in the coming days;[17] or even using the SARS-CoV-2 concentrations in wastewater to estimate prevalence in a community.[19] The latter application requires a clear understanding of fecal shedding dynamics over the course of the illness, which is not yet established.

Received: September 14, 2020
Revised: November 16, 2020
Accepted: November 18, 2020
Published: December 7, 2020

Table 1. Inventory of Samples Used in This Study[a]

date	influent POTW A (Palo Alto)	solids POTW A	influent POTW B (San Jose)	solids POTW B	solids POTW B (RNeasy)	solids POTW B two-step dd-RT-PCR for N1/N2
3/22/20	X	X	X	X	X	X
3/23/20			X	X		
3/25/20	X	X	X	X	X	X
3/29/20	X	X	X	X	X	X
3/30/20			X	X		
4/1/20	X	X	X	X	X	X
4/15/20	X	X	X	X	X	X

[a]Unless specified in the column name, samples were processed using RT-QPCR and ddRT-PCR for N1 and N2 and RT-QPCR for PMMoV and BCoV. Unless otherwise specified, solids samples were extracted using the powerfecal kit.

Many early studies on SARS-CoV-2 in wastewater have focused on wastewater influent. When detected in influent, viral particles are first concentrated with either a filtration method[18] or an organic flocculation method[20] and then the SARS-CoV-2 genome is targeted with a PCR-based method. In an earlier study, enveloped viruses mouse coronavirus murine hepatitis virus MHV and bacteriophage Phi6 partitioned to a greater extent to wastewater solids in wastewater influent than nonenveloped bacteriophages MS2 and T3.[21] The partition coefficients from that study were 1500, 1200, and 270 mL/g for MHV, Phi6, and MS2, respectively. These results suggest that wastewater solids may contain coronaviruses at concentrations 1000 times those found in influent, on a per mass basis, and that monitoring solids could lead to more sensitive detection of SARS-CoV-2.[22] Indeed, human coronaviruses HKU1 and 229E were previously detected in residual biosolids with metagenomic sequencing.[23]

In this study, we compared SARS-CoV-2 concentrations recovered from paired wastewater influent and primary settled solids collected at two different wastewater treatment plants collected on 5−7 days during a rising limb of the outbreak using different analytical methods. Subsequently, we applied refined methods to near daily samples of primary settled solids at a wastewater treatment plant over 89 days to investigate how SARS-CoV-2 concentrations in solids tracked COVID-19 cases in the sewershed. In addition to quantifying two SARS-CoV-2 RNA targets (N1 and N2), we quantified coronavirus recovery and wastewater fecal strength in every sample using bovine coronavirus (BCoV) and pepper mild mottled virus (PMMoV), respectively. Although the work focuses on a single pandemic virus, the results will be relevant for a wide suite of viral targets that have an affinity for solids.

METHODS AND MATERIALS

Sample Collection and Storage. Influent and primary settled solids were collected from two publicly owned treatment works (POTWs), hereafter referred to as POTW A (Palo Alto Regional Water Quality Control Plant) and POTW B (San José-Santa Clara Regional Wastewater Facility), both located in Santa Clara County, California, USA. POTW A and B serve populations of 0.2 and 1.5 million, respectively, with permitted flows of 39 and 167 million gallons per day, respectively. POTW B adds $FeCl_3$ to its waste stream (10 mg/L) prior to the headworks for odor control. The residence time of settled solids in the primary clarifier is estimated to be between 2 and 14 h for POTW A and between 1 and 2 h for POTW B.

From both plants, 50 mL of influent was collected at the headworks as 24 h flow-weighted composite samples and 50 mL of settled solids samples were collected from the primary settling tank. Grab samples of settled solids were collected from POTW A, and 24 h composite settled solids samples were collected from POTW B. The 24 h composite solids samples from POTW B were collected by compositing 500 mL from the primary sludge line every 4 h. Samples were collected in 10% HCl acid-washed plastic containers. Storage conditions are described in the Supporting Information.

Paired influent and solids samples were collected at both POTWs on the following dates: March 22, March 25, March 29, April 1, and April 15, 2020. Additional dates were included for POTW B (March 23 and March 30) (Table 1). Dates were chosen to span a high prevalence period in the initial phase of the pandemic. These samples are hereafter referred to as "method evaluation samples".

A longitudinal collection of primary settled solids was obtained from POTW B. Eighty-nine samples were collected daily from March 16 to May 31 and three times a week from June 2 to July 12, using the same collection techniques as the method evaluation samples. Hereafter, these are referred to as "longitudinal samples". We did not have access to samples collected prior to the pandemic for comparison.

Influent Preanalytical Processing. Immediately prior to analysis, frozen influent samples were transferred to 4 °C until thawed (range: 12−48 h). Between 43 and 45 mL of influent was centrifuged at 24,000*g* for 15 min at 4 °C to pellet solids. The resultant clarified supernatant (40 to 42 mL) was decanted, and viruses were concentrated from the supernatant by a PEG precipitation method.[21] This method was selected after preliminary head-to-head testing of PEG precipitation and centrifugal ultrafiltration to concentrate viruses from influent yielded comparable recovery results for N1 and N2 (Figure S1), and because we anticipated, there would be fewer pandemic-related supply chain issues with the PEG method. MHV strain A59 and PMMoV were used as an exogenous and endogenous recovery controls, respectively. PMMoV also served as a fecal strength control. An attenuated vaccine strain of bovine coronavirus (BCoV) was used as a nucleic acid extraction positive control; it was spiked into the viral concentrate before it was subjected to nucleic acid extraction using Qiagen AllPrep PowerViral DNA/RNA kits and further

https://dx.doi.org/10.1021/acs.est.0c06191
Environ. Sci. Technol. 2021, 55, 488−498

purification using Zymo OneStep PCR inhibitor removal columns (Zymo Research, Irvine, CA). Further details are in the Supporting Information.

Solid Preanalytical Processing. Immediately prior to analysis, frozen solids samples were transferred to 4 °C until thawed (range: 12−48 h). Thawed solid samples (35−53 mL) were centrifuged at 24,000*g* at 4 °C for 30 min, and the supernatant was decanted. Percent solids was measured for concentrated solids samples by placing sample aliquots in preweighed aluminum weigh dishes and weighing the sample before and after drying at 105 °C for 24 h.

The method evaluation solids samples were divided to test two different extraction processes: for the first, 0.2−0.4 g of sample was aliquoted for extraction with the Qiagen AllPrep PowerFecal DNA/RNA kit ("powerfecal" kit), and for the second, 1.8−2.8 g of sample was aliquoted for extraction with the RNeasy PowerSoil total RNA kit ("RNeasy" kit). Aliquots were spiked with BCoV as an extraction recovery control. Two extraction replicates were completed per sample (two powerfecal and two RNeasy extractions per POTW per time point). Nucleic acids were further purified using Zymo OneStep PCR inhibitor removal columns (Zymo Research, Irvine, CA). Further details are in the Supporting Information.

For the longitudinal solids samples, RNA was extracted using the RNeasy kit and purified with the Zymo inhibitor removal kit using the same protocol described above with two modifications:[24] (1) after step 9 in the kit's instructions, samples were stored overnight at −20 °C; and (2) positive pressure was used per manufacturer's instructions to aid flow through columns. Seven of the 89 samples were extracted in duplicate, and extraction blanks were run with each sample batch. Samples were randomized and blinded to laboratory technicians prior to analysis.

RT-QPCR. For method evaluation samples, PMMoV, MHV, BCoV, and SARS-CoV-2 N1 and N2 were quantified using two-step RT-QPCR. Preliminary experiments suggested that the RT step was inhibited, so dilutions of the extract were used as templates for the RT step (see the Supporting Information for details). For influent, undiluted and 1:10 diluted RNA were used as templates; for solids, undiluted, 1:10, and 1:50 diluted RNA were used as templates. Each template was run in triplicate, and triplicate reactions were pooled prior to QPCR.

Resultant cDNA was used as the template in QPCR assays targeting PMMoV, MHV, BCoV, and SARS-CoV-2 N1 and N2 (primers and probes in Table S1) using an ABI StepOnePlus instrument (Thermo Fisher Scientific, Waltham, MA). All templates were run in duplicate. Standard curves were run in duplicate on each plate using cDNA standards (see the Supporting Information) at concentrations from 3 to 3×10^5 copies/reaction; duplicate NTCs were included on each plate. Concentrations per reaction were converted to copies per volume of influent or per g of dry solid weight using dimensional analysis (calculation details in the Supporting Information). Samples were considered "below the limit of quantification" (BLOQ) if the Cq value of the sample was higher than that of the lowest cDNA standard, but less than 40, or if the targets in both technical replicates did not amplify within 40 cycles. Concentrations of unknown samples were calculated using plate-specific standard curves. Additional details are in the Supporting Information.[25]

ddRT-PCR. RNA from the method evaluation samples was used as the template in one-step digital droplet (dd)RT-PCR for N1 and N2 SARS-CoV-2 targets using BioRad SARS-CoV-2 droplet digital PCR kits (cat. no.: 12013743; Hercules, CA) and a BioRad QX200 AutoDG droplet digital PCR system. Technical duplicates were run (two wells); wells were merged for data analysis. To test for inhibition, each template was run at two dilutions: undiluted and 1:10 dilution. A positive control consisting of SARS-CoV-2 RNA isolated from a nasopharynx swab of a high-titer patient from Stanford Hospital and NTCs were run on each plate in duplicate. The choice of this positive control avoided supply chain issues associated with a commercially available control and was available free of charge. QuantaSoft and QuantaSoft Analysis Pro (BioRad) were used to manually threshold and export the data (see the Supporting Information for additional details on thresholding). The required number of droplets for a sample with merged duplicate wells was at least 10,000. In order for a sample to be scored as positive, three or more positive droplets were required in the merged wells. Concentrations per reaction were converted to copies per volume of influent or per g of dry weight using dimensional analysis.

A two-step ddRT-PCR assay for N1 was also trialed using a subset of the method evaluation samples. RNA was stored at −80 °C for up to 5 days between running the one-step and two-step assays, to minimize the potential for RNA degradation during storage (see the Supporting Information).

For the longitudinal samples, the one-step ddRT-PCR duplex assay for N1 and N2 and a duplex assay for PMMoV and BCoV[26] were used. N1 and N2 were quantified in undiluted and 1:10 diluted templates; BCoV and PMMoV were quantified in 1:10 and 1:1000 diluted templates. The N1/N2 duplex assay was conducted in triplicate wells, and the BCoV/PMMoV duplex assay was conducted in duplicate wells. The replicate wells were merged for data analysis. Positive N1/N2 and negative controls and threshold setting for the longitudinal samples were conducted as described for the method evaluation samples. The positive control for BCoV was a direct extraction of reconstituted BCoV vaccine diluted to 10^6 cp/mL, and the positive control for PMMoV was a synthetic DNA ultramer. In addition, a pooled matrix control was run on every N1/N2 duplex assay plate. This was created by adding equal-volume aliquots of each sample on the plate to one tube and spiking this pooled matrix with clinical SARS-Cov-2 RNA. Additional details of ddRT-PCR[27] can be found in the Supporting Information and Table S7.

COVID-19 Epidemiology Data. The number of new clinically confirmed COVID-19 cases within the sewershed of POTW B was obtained using georeferenced case data and a POTW-provided shapefile of their service area in ArcGIS. The date stamp is that of specimen collection. As data were handled and provided by the county, no IRB approval was needed.

Statistics. Statistics were computed using Microsoft Excel and RStudio (version 1.1.463). Paired and unpaired *t* tests were used to compare groups after confirming that data were normally distributed. For calculating recoveries and making numerical comparisons across samples using the high copy number targets measured by RT-QPCR (PMMoV, MHV, and BCoV), the results from reactions that yielded the highest measured concentration were used to balance loss of the signal against effects of inhibitory substances. By calculating recovery in this way, we assume that inhibition has been alleviated. For ddRT-PCR data, "total error" from merged wells is reported in the form of standard deviations. Pearson correlation coefficients assessed association between different measurements among samples.

https://dx.doi.org/10.1021/acs.est.0c06191
Environ. Sci. Technol. 2021, 55, 488−498

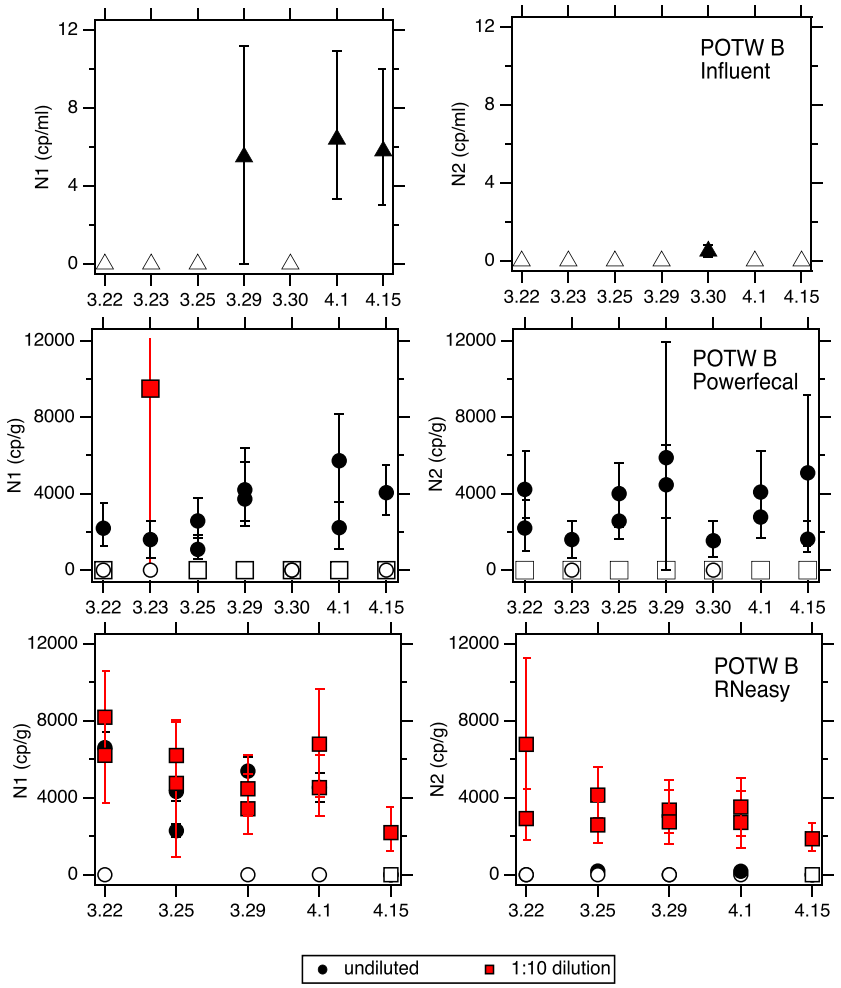

Figure 1. N1 and N2 measured at POTW B using ddRT-PCR. Top row: concentrations in influent in units of copies (cp) per mL. Middle row: concentrations in solids extracted using the powerfecal kit in units of cp per g of dry weight. Bottom row: concentrations in solids extracted using the RNeasy kit in units of cp per g of dry weight. Open symbols indicate those where no target was detected (less than three positive droplets). Error bars represent standard deviations as represented by the "total error", which includes the Poisson error and differences among merged wells. Results for undiluted and 1:10 diluted templates are provided for the solids; results for influent are for the 1:10 diluted template for N1 and the undiluted template for N2—results for influent dilutions not shown are all nondetects.

We used a resampling-based strategy to evaluate whether the observed measurements N1 and N2 with and without PMMoV normalization were predictive of clinically confirmed COVID-19 cases in the sewershed of POTW B. First, we applied first differencing to account for autocorrelation in data series.[28] We then carried out a linear regression (using N1 as the example): $\text{cases}_t - \text{cases}_{t-k} = m^*(\text{N1}_t - \text{N1}_{t-k})$ where m is the regression coefficient describing the rate of change of cases with respect to RNA target concentration, the subscript t indicates the day of measurement, and k is the number of days used for differencing. We used $k = 7$, but we also used $k = 14$ to determine if results were sensitive to the choice of k. If an N1 or N2 concentration data point was missing at day $t - k$, then the value for the closest previous date was imputed. To account for the technical variability of the wastewater measurements, empirical p values and regression coefficients m were determined using 1000 bootstrap resamplings. The observed top and bottom confidence bounds of each measurement were used to define a uniform distribution, which was resampled randomly within each bootstrap replicate. For samples below the detection limit, we used random sampling of a uniform distribution bounded by 0 and the lower detection limit (estimated at 40 copies/g of dry weight). In addition to raw case counts, a 7 day smoothed case data set was also used as the dependent variable. A downsampling analysis was also conducted to investigate the frequency of sample collection needed to observe associations between case counts and wastewater data. We downsampled the case and wastewater data to fortnightly, weekly, and twice per week frequencies using a random nonmissing observation within each appropriate period and examined as described above except that k for biweekly was 2 or 4 half-weeks, and for weekly and fortnightly, k was 1 or 2 (weeks/fortnights).

RESULTS

Analytical Controls and Assay Performance. NTCs and extraction blanks were negative for all targets in all analytical methods. QPCR assay efficiencies ranged from 78 to 105%, and standard curve R^2 ranged from 0.98 to 0.99 (Table S2 and Figure S2).

Method Evaluation: Comparison of RT-QPCR versus ddRT-PCR Assays on Influent and Settled Solids. With RT-QPCR, N1 and N2 were not detected in any influent sample, even when the RNA template was diluted 1:10 and

https://dx.doi.org/10.1021/acs.est.0c06191
Environ. Sci. Technol. 2021, 55, 488−498

cDNA was diluted 1:10, except for a single influent from POTW B (Table S3) that resulted in detection below the limit of quantification. When one-step ddRT-PCR was applied to the same undiluted and 1:10 diluted RNA templates, one sample tested positive for N1 in POTW A, three tested positive for N1 at POTW B, and one tested positive for N2 in POTW B (Table S4). In all but one of the samples that resulted in positive measurements, the undiluted template yielded a nondetect, suggesting inhibition of the reactions in the undiluted template.

For solids samples extracted with powerfecal kits and analyzed with RT-QPCR, SARS-CoV-2 targets were detected in at least one replicate from one of five samples from POTW A and four of seven samples from POTW B (Table S3). Detection was inconsistent across extraction and technical replicates, and there was no case where both extraction and technical replicates were positive. When analyzed with ddRT-PCR, the SARS-CoV-2 targets were detected and quantified in zero out of five POTW A solids samples and seven out of seven POTW B samples (Table S4). ddRT-PCR results were more consistent across extraction replicates than RT-QPCR (Figure 1 and Table S4).

The improved performance of the ddRT-PCR method compared to the RT-QPCR method for both influent and solids samples was unlikely due to differences in template amounts. The virtual influent volumes in RT-QPCR and ddRT-PCR assays were 2 and 8.4 mL, respectively (when the template was not diluted); and for solids, the virtual wet masses of solid assays in the RT-QPCR and ddRT-PCR reactions were 20 and 50 mg, respectively (when the template was not diluted); thus, theoretical lower detection limits are similar across analytical approaches (Table S5). There are several possible explanations for the low and inconsistent detection of SARS-CoV-2 targets in influent and solids with RT-QPCR, including assay inhibition, and the absence or low occurrence of viral RNA in the samples. We studied RT-QPCR inhibition in more depth using endogenous PMMoV and spiked MHV and BCoV (Figure S3). The results demonstrate inhibition for the RT-QPCR assays of endogenous and exogenous recovery targets despite efforts to alleviate it using the Zymo OneStep inhibitor removal columns and dilution of the template. For influent, PMMoV and MHV concentrations were generally the highest when the RNA template was diluted 1:10 prior to RT, compared to results from undiluted and 1:10 diluted cDNA generated from the undiluted RNA template (Figure S3). This suggests that the RT step, not the PCR step, was most inhibited for the PMMoV and MHV RT-QPCR assays. For solids, extract dilutions of 1:50 appeared to alleviate inhibition for RNA obtained from POTW A (Figure S3 and Table S6). For solids from POTW B, however, inhibition may not have been alleviated even after a 1:50 dilution.

Based on these results comparing the performance of the RT-QPCR and ddRT-PCR methods and the improved sensitivity of the ddRT-PCR methods, we selected the ddRT-PCR methods for further SARS-CoV-2 analysis.

Method Evaluation: Comparison of RNeasy and Powerfecal Extraction Kits and One-Step versus Two-Step ddRT-PCR for Settled Solids. We used the SARS-CoV-2 ddRT-PCR assays and the POTW B solids to compare powerfecal and RNeasy solid extraction kits. The virtual wet masses of solids assayed in the duplicate merged wells were approximately 50 mg (powerfecal) and 250 mg (RNeasy) when the templates were not diluted (theoretical detection limits shown in Table S5). Samples treated with the powerfecal kit were more commonly positive for SARS-CoV-2 targets in the undiluted template than in the 1:10 diluted template (Figure 1). By contrast, samples treated with the RNeasy kit were positive for SARS-CoV-2 at both dilutions, but detection was more consistent with the 1:10 diluted templates (Figure 1). The SARS-CoV-2 target concentrations were similar across the extraction replicates, and the null hypothesis that paired replicates have the same concentration was not rejected ($p > 0.05$ for all four comparisons (two targets × two RNA extraction kits), paired t test). The concentrations of N1 and N2 measured in the same sample replicate were not different between the two kits (paired t test, $p > 0.05$). Although the powerfecal kit samples less material than the RNeasy kit, these results suggest that some of the RNeasy kit extracts require a 1:10 dilution, thus negating the advantages of the extra sample mass.

Whereas the N1 target was detected in every solid sample from POTW B when the one-step ddRT-PCR assay was employed (Figure 1), it was not detected when a two-step ddRT-PCR assay was conducted (all samples were non-detects). This result, along with results presented earlier for two-step RT-QPCR, suggests that two-step assays may not work effectively on these samples.

Method Evaluation: Comparison of SARS-CoV-2 RNA Concentrations Measured in Influent and Primary Settled Solids. We compared SARS-CoV-2 measurements made in influent and solids samples collected on the same days at POTW B (Figure 1). Solid results obtained using the powerfecal kits are used for the comparisons. At POTW B, the N1 target was detected in three out of seven influent samples and six out of seven solids samples and the N2 target was detected in one out of seven influent samples and seven out of seven solids samples. The N1 target was quantified in both influent and primary solids on three dates (3/29, 4/1, and 4/15), and the N2 target was quantified in both influent and primary solids on one date (3/30). The ratio of N1 solid concentrations (cp/g; mean of replicates) to influent concentrations (cp/mL) on the three dates was 720, 620, and 350 mL/g, respectively. For the N2 target, the ratio was 3100 mL/g. These results suggest that on a per mass basis, these targets are present at between ∼100 and ∼1000 higher concentrations in solids.

Method Evaluation: Recovery of Viral Targets through Preanalytical Processing. Recovery measurements help characterize preanalytical method consistency across samples. For the influent method, we measured the recoveries of endogenous PMMoV and spiked MHV through the PEG concentration method (Figure S4). The median PMMoV recovery was 21% (range: 8 to 30%), and the median MHV recovery was 7% (range: 2 to 16%). The MHV recovery was lower than that for PMMoV by, on average, 13% (paired t test, $p < 0.05$). We used BCoV to assess recovery specifically through nucleic acid extraction and purification and through inhibitor removal steps. Recoveries of BCoV through these steps ranged from 3 to 48% (median = 26%). The PEG concentration step and nucleic acid extraction/purification step are conducted in series. Assuming that the BCoV extraction recoveries apply to all viral targets, our results suggest that viral recoveries are between 0.1 and 7% (median 1%, based on MHV) or between 1 and 8% (median 7%, based on PMMoV) of actual influent concentrations.

https://dx.doi.org/10.1021/acs.est.0c06191
Environ. Sci. Technol. 2021, 55, 488−498

There were no significant differences in recoveries of PMMoV, MHV, and BCoV in influent between the two POTWs (t test, $p > 0.05$) or in samples that were positive or negative for N1 or N2 (t test, $p > 0.05$). In fact, the influent sample with one of the lowest MHV and BCoV recoveries (POTW B on 3/29/20) was one of the few influent samples positive for N1.

PMMoV may serve not only as a process control but also as a means of assessing the "fecal strength" of sewage. PMMoV measured in the viral concentrate varied between 7.7×10^2 and 7.0×10^3 copies/mL of influent across plants (Figure S4). There was no significant difference in PMMoV influent concentrations between plants ($p > 0.05$).

Method Evaluation: Endogenous and Spiked Virus Recoveries in Solids from Method Evaluation Study. There was no viral concentration step in the solid methods, and BCoV served as an extraction recovery control. BCoV recovery varied from 0 to 33% (median = 16%) using the powerfecal kit and from 0 to 10% (median = 4%) using the RNeasy kit (Figures S5 and S6). The 0% recovery values were obtained in POTW B solids collected on April 15 and treated with the RNeasy kit and POTW B solids collected on March 25 and treated with the powerfecal kit. Interestingly, PMMoV and SARS-CoV-2 targets were measured in the same extracts with 0% BCoV recovery at concentrations not largely different from other dates. The measured BCoV recoveries were not different across plants or across extraction kits (t test, $p > 0.05$). It is possible, however, that the BCoV recoveries in the POTW B solids are underestimates because we are not certain that the RT-QPCR assay conducted at the highest extract dilution was free of inhibition.

PMMoV levels in solids from POTW A and POTW B varied between 5×10^4 and 7×10^7 copies/g of dry weight (median: 2×10^6 copies/g) when extracted with the powerfecal kit (Figure S6). Only samples from POTW B were measured with the RNeasy extraction kit, and the resulting concentrations ranged from 5×10^5 to 3×10^6 copies/g of dry weight (median: 1×10^6 copies/g; Figure S5). These concentrations are twice as high, on average, as those measured using the powerfecal templates (paired t test, $p < 0.05$). The PMMoV concentrations may be underestimates due to unresolved assay inhibition. Concentrations of PMMoV were not different across extraction replicates regardless of which extraction kit was used (paired t test, $p > 0.05$). PMMoV concentrations measured in solids at POTW A were not different from those measured at POTW B (t test, $p > 0.05$, data from powerfecal extracts).

Sample-to-sample differences in BCoV or PMMoV RNA recovery or fecal strength might affect measurements of N1 and N2. Assuming PMMoV concentration is a proxy for recovery and/or fecal strength, we tested whether N1 or N2 concentrations are correlated with PMMoV concentrations and BCoV recovery. N1 and N2 concentrations in solids are not correlated to BCoV recovery or PMMoV concentrations regardless of the extraction kit used ($p > 0.05$) (Figures S5 and S6).

Longitudinal Data from POTW B. The method performance experiments demonstrated that the primary solid method resulted in more positive and consistent SARS-CoV-2 signals than the influent method. Furthermore, we found that the one-step ddRT-PCR assay performed on the solid extracts resulted in more positive results than the two-step RT-QPCR and two-step ddRT-PCR assays. We therefore focused our longitudinal analysis on primary settled solids samples from POTW B using the RNeasy kit and ddRT-PCR for measuring all targets (Figure 2). Concentrations of N1 and N2 in each sample were

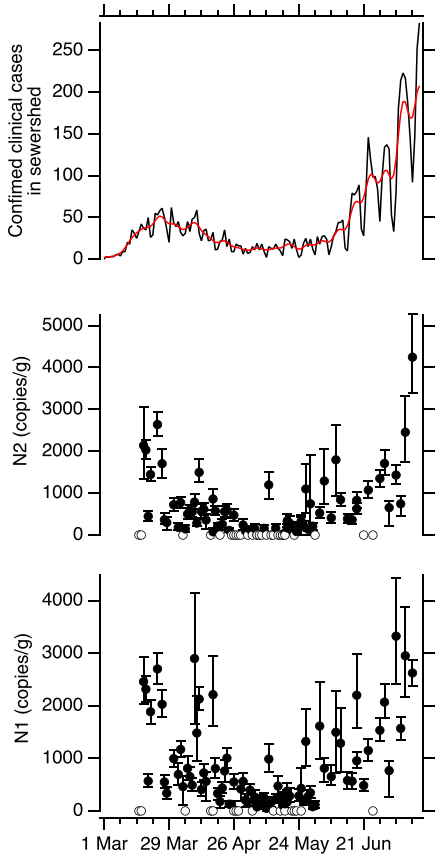

Figure 2. Top panel: confirmed new cases of COVID-19 in the sewershed of POTW B (black) and 7 day smoothed new cases (red). Middle and bottom panels: concentrations of N1 and N2 measured in solids (copies per g of dry weight). Error bars are standard deviations as total errors from the ddPCR machine. Open symbols are nondetects plotted at 0. The theoretical lowest concentration measurable is ~40 copies/g of dry weight. N1 and N2 normalized by PMMoV can be found in Figure S8.

derived from the one-step ddRT-PCR reactions that used the undiluted RNA template unless those that used the 1:10 diluted template produced a concentration higher than the upper standard deviation for the undiluted template (10/96 and 6/96 samples required 1:10 dilution for N1 and N2, respectively).

N1 and N2 were detected in 79 and 68 of the 96 samples, respectively. When detected, average N1 and N2 values were 870 and 730 cp/g with maximums of 3330 and 4250 cp/g, respectively (Figure 2). Replicate extractions generally yielded concentrations that were similar.

Median PMMoV was 2×10^7 cp/g (interquartile range: 1×10^7 to 4×10^7 cp/g) (Figure S7), suggesting fairly constant fecal strength of the solids. We normalized measured concentrations of N1 and N2 to obtain fecal strength normalized target concentrations to include in the statistical analyses (Figure S8). The recovery of BCoV was similar for the longitudinal samples to the method evaluation samples, with a median recovery of 3% (interquartile range: 1 to 5%) (Figure S7). We omitted the N1 and N2 data from our data set for the one sample where 0% BCoV recovery was measured (March

https://dx.doi.org/10.1021/acs.est.0c06191
Environ. Sci. Technol. 2021, 55, 488−498

16). BCoV recovery was higher than 10% on 8 days; N1 and N2 concentrations were not significantly different on those days compared to the others ($p > 0.05$). Longitudinal data are available through the Stanford Digital Repository.[29]

The concentrations of N1 and N2 tracked the reporting of new cases in the sewershed (based on specimen collection date) when accounting for autocorrelation and technical errors associated with the wastewater measurements (using raw case counts, $m = 0.024$ cases/copies/g for both N1 and N2, $p = 0$ and 0.005, respectively). Results were not sensitive to the choice of k, smoothing of case data, or normalization of N1 and N2 by PMMoV to account for changing sample-to-sample differences in fecal strength or recovery (Table S8). Downsampling wastewater data collection and analysis frequency to twice per week yields significant associations between case counts and wastewater concentrations; however, when downsampled to fortnightly or once per week, associations were no longer significant (Table S8).

DISCUSSION

Our results suggest that testing wastewater solids for SARS-CoV-2 may be more sensitive than testing influent. We detected co-occurring SARS-CoV-2 N1 and N2 targets in nearly every solid sample tested at POTW B, yet both targets were never co-detected in influent samples. The lack of detection of SARS-CoV-2 targets at POTW A in both influent and solids may be a result of low prevalence of COVID-19 in its sewershed; on the days that POTW A samples were tested there were between 1 and 10 clinically confirmed new COVID-19 cases in its sewershed compared to between 22 and 62 cases in the POTW B sewershed on the same days. The measured ratios of N1 and N2 concentrations in solids and influent were between 350 and 3100 mL/g; these values are likely low estimates as the influent N1 and N2 concentrations were below our detection limit in most of the samples from many days when N1 and N2 were detected in solids. Depending on the preanalytical method used in our study (i.e., extraction kit, template dilution factor, etc.), there was between 20 and 1100 times more influent than dry solids on a per mass basis in the PCR reactions (Table S5). However, solids have, at minimum, between 350 and 3100 times higher concentrations than influent on a per mass basis based on the measurements we made in this study, consistent with those reported by Ye et al.[21] As a result, the number of target copies could be much higher in the PCR reactions for solids compared to influent. The increased sensitivity in detecting SARS-CoV-2 in solids will be particularly important for screening communities at the sewershed scale for outbreaks occurring within communities with low levels of COVID-19 prevalence. Other viruses have a high affinity for wastewater solids including adenovirus, rotavirus, and various enteroviruses,[30−33] so solids are likely to be useful for WBE applied to other viral diseases. We also note that solid analysis avoids the preconcentration step necessary with influent analysis. It should be noted that POTW B added $FeCl_3$ to its influent. While it has been documented in other work that SARS-CoV-2 RNA can be enriched in solids[22,34] from other POTWs, we cannot rule out that the addition of the flocculant could have influenced the partitioning of the virus/RNA between wastewater solids and liquid as well as the virus recoveries with our methods. Research is underway to gain additional insight into partitioning of SARS-CoV-2 RNA.

Using longitudinal samples from POTW B, we identified a positive association between N1 and N2 in solids and the number of new COVID-19 infections. A similar result was reported by Peccia et al.[22] for a POTW on the east coast of the US. When N1 and N2 are normalized by fecal strength, as determined by PMMoV, associations were similar. Additional work is needed to better understand when normalization of SARS-CoV-2 RNA concentrations by PMMoV concentrations may be useful; we suspect that it may be useful for comparing measurements made at different plants, at the same plant across times when the waste stream varies in fecal strength, or using different methods that have differing recoveries. Whether the N1 and N2 signals signals temporally lead the new case data is complicated by data autocorrelation, evaluating data from multiple POTWs may improve robustness of such signal-lead analyses. The positive associations suggest that SARS-CoV-2 RNA in solids can be used to confirm trends in infection prevalence and, therefore, augment case data to inform a response to the COVID-19 pandemic.

Ideally, wastewater surveillance could take place with high-resolution sample collection (e.g., daily); however, this may not be possible for many utilities/communities due to limited staffing, supplies, and resources. Our downsampling analysis suggests that sampling solids twice per week would be frequent enough to identify the global trends in the clinical case data. It is important to note that case data are imperfect as testing availability, population testing bias, and time to testing result can vary substantially. For example, during the initial phase of the pandemic (between mid-March and mid-April), clinical testing was not widely available to people residing in the sewershed; however, sentinel surveillance efforts suggest that during this time, there was transmission in the community.[35] While prevalence in the sewershed during this period is unknown given limited testing, solid concentrations of N1 and N2 are just as high during the initial infection peak as during the second infection peak; this may suggest that infection prevalence during the two confirmed case peaks was similar.

Whereas Peccia et al.[22] recently reported correlations between N1 and N2 in settled solids and new COVID-19 cases during a period when infections were rising, we report correlations across both rising and falling periods of the epidemiological curve. Given that individuals likely shed SARS-CoV-2 for weeks,[36,37] it is somewhat surprising that SARS-CoV-2 RNA concentrations correlate with the number of new COVID-19 infections. This result may yield insight into the time course and magnitude of fecal shedding and is consistent with substantially higher shedding rates during the initial phase of the infection.[38] More fecal shedding data are needed, especially for presymptomatic individuals to fully understand if SARS-CoV-2 RNA concentrations in solids can be linked quantitatively to prevalence of infection in the sewershed.

The RNA extraction, concentration, and purification procedures used in this study did not eliminate RT and PCR inhibition despite the use of clean-up kits. Dilution of templates was needed, at times, for both influent and solids to obtain signals, even when using ddRT-PCR, which is known to decrease the effects of inhibition in some cases.[39,40] Wastewater is a diverse, complex matrix that differs chemically and biologically between POTWs. The presence of metals, organics, and other materials can impede the reverse transcription and PCR.[41] The solids from POTW B appeared to be more inhibited than those from POTW A, likely because they contain Fe-containing compounds as a result of their

https://dx.doi.org/10.1021/acs.est.0c06191
Environ. Sci. Technol. 2021, 55, 488−498

$FeCl_3$ addition, a known PCR inhibitor.[42] These results highlight the importance of testing for inhibition in wastewater matrices and also the need for more research on how to alleviate inhibition without diluting the extracts.

We used recovery controls in our analyses including an endogenous, nonenveloped virus (PMMoV) and two beta coronaviruses (MHV and BCoV). The recoveries we report are similar to those reported by others.[43−46] We did not correct concentrations reported in this study using measured recoveries as there is great uncertainty regarding whether a recovery surrogate mimics the behavior of the virus of interest—in this case, SARS-CoV-2, even if it shares certain biological characteristics. It is impossible to know confidently that the spiked recovery target will interact with the components of the matrix in the same manner that an endogenous target interacts. In addition, it is not known whether the spiked recovery control mimics the state of the endogenous SARS-CoV-2 targets as it is unknown whether the SARS-CoV-2 virus exists as an intact virion in the sewage matrices, or if its lipid envelope is absent, or if its RNA is located outside of the capsid. In light of all these complexities, we believe that recovery of a surrogate should be used to ensure that sample processing is not "out of the ordinary" and can be used to identify problems during sample processing. Indeed, during the longitudinal sample processing, we identified one sample where the BCoV recovery control failed and removed that sample's data from subsequent statistical analysis.

It was necessary to freeze the samples prior to analysis due to logistical and sample throughput constraints. Each sample underwent a freeze−thaw cycle prior to processing; a freeze−thaw may impact RNA levels in a sample and may impact RNA in influent and solids differently. Additional work will be required to investigate these issues.

The amount of feces or urine in wastewater may vary with time based on sewershed populations, precipitation, changing waste streams, or human behaviors.[47] Such variation may affect targets relative to WBE and, in this case, SARS-CoV-2 RNA. Normalization refers to the normalization of a WBE target by another wastewater target that is a measure of the amount of fecal material in the wastewater. Normalization is not a practice that has been extensively tested in environmental virology. However, it has been explored in the use of wastewater-based epidemiology for drug use.[47−49] We tested PMMoV as a normalization factor as it is found extensively in wastewater globally and it originates in human feces.[50] PMMoV concentrations measured in the influent and solids of the plants we sampled did not vary substantially across samples or plants,[50] suggesting limited changes to the fecal content of the waste stream during the study. This may explain why normalizing N1 and N2 by PMMoV did not substantially change correlations with new COVID-19 cases in the sewershed.

Implications and Future Work. Solids naturally concentrate SARS-CoV-2, making it a reliable target for WBE. However, there are situations where solid analysis may be impractical. For example, in POTWs with no primary settling step or for sewage sampling from manholes within a sewershed, a sufficient mass of solids may be difficult to collect.

There are several avenues of research needed to further understand the limitations and utility of WBE for COVID-19. First, more information is needed about the decay of viral targets both in influent[51] and within solids. This information is needed to better understand how infection in the sewershed affects concentrations in wastewater matrices. Second, the degree to which settled solids represent a natural composite sample owing to mixing processes in the settling tank would be useful. While composite samples of influent are preferred over grab samples owing the changes in the influent stream with time,[52] the same may not be true for settled solids, eliminating the need for composite samplers. Importantly, additional information on duration and magnitude of shedding of viral RNA via feces is needed; also, the extent to which viral RNA is encapsulated versus extraviral in feces and sewage is needed to predict its fate and transport in the waste stream.

■ ASSOCIATED CONTENT

Supporting Information

The Supporting Information is available free of charge at https://pubs.acs.org/doi/10.1021/acs.est.0c06191.

Materials and methods; assay primers, probes, and conditions for all PCR assays; summary of QPCR assay efficiencies and R^2 of standard curve regression; RT-QPCR results for N1 and N2 SARS-CoV-2 targets; ddRT-PCR results for N1 and N2 SARS-CoV-2 targets; theoretical detection limits for N1 and N2 assays; average and standard deviations of ΔCq for different dilutions of RNA for solids samples; details for essential and desired information as requested in the updated dMIQE guidelines; comparison of recovery of spiked SARS-CoV-2 RNA from PEG precipitation and ultrafiltration methods to concentrate influent samples; representative QPCR standard curves for each assay used during method optimization experiments for influent and solids; RT-QPCR results for endogenous (PMMoV) and exogenous (BCoV and MHV) recovery targets at different dilutions to test for inhibition; mean concentrations of qPCR technical replicates of PMMoV in concentrated influent samples and mean recoveries of MHV and BCoV spike-in surrogates; N1, N2, PMMoV, and recovery of BCoV in solids from POTW B in each biological replicate using data from the RNeasy kit; N1, N2, PMMoV, and recovery of BCoV in solids from POTWs A and B in each biological replicate using data from the powerfecal kit; recovery of BCoV and PMMoV concentrations for the longitudinal samples; N1 and N2 normalized by PMMoV; and examples of ddRT-PCR experimental results for a no template control, a representative sample, and a positive control containing SARS-CoV-2 RNA isolated from clinical samples or PCR standards (PDF)

Results from statistical models (XLSX)

■ AUTHOR INFORMATION

Corresponding Authors

Krista R. Wigginton − *Department of Civil and Environmental Engineering, University of Michigan, Ann Arbor 48109, Michigan, United States;* orcid.org/0000-0001-6665-5112; Phone: (734) 763-2125; Email: kwigg@umich.edu

Alexandria B. Boehm − *Department of Civil and Environmental Engineering, Stanford University, Stanford 94305, California, United States;* orcid.org/0000-0002-8162-5090; Phone: 650-724-9128; Email: aboehm@stanford.edu

https://dx.doi.org/10.1021/acs.est.0c06191
Environ. Sci. Technol. 2021, 55, 488−498

Authors

Katherine E. Graham − *Department of Civil and Environmental Engineering, Stanford University, Stanford 94305, California, United States*

Stephanie K. Loeb − *Department of Civil and Environmental Engineering, Stanford University, Stanford 94305, California, United States*

Marlene K. Wolfe − *Department of Civil and Environmental Engineering, Stanford University, Stanford 94305, California, United States*

David Catoe − *Joint Initiative for Metrology in Biology, SLAC National Accelerator Laboratory, Stanford 94305, California, United States*

Nasa Sinnott-Armstrong − *Department of Genetics, Stanford University School of Medicine, Stanford 94305, California, United States; Emmett Interdisciplinary Program in Environment and Resources, Stanford University, Stanford 94305, California, United States*

Sooyeol Kim − *Department of Civil and Environmental Engineering, Stanford University, Stanford 94305, California, United States*

Kevan M. Yamahara − *Monterey Bay Aquarium Research Institute, Moss Landing 95039, California, United States*

Lauren M. Sassoubre − *Department of Engineering, University of San Francisco, San Francisco 94117, California, United States;* orcid.org/0000-0001-5105-9529

Lorelay M. Mendoza Grijalva − *Department of Civil and Environmental Engineering, Stanford University, Stanford 94305, California, United States*

Laura Roldan-Hernandez − *Department of Civil and Environmental Engineering, Stanford University, Stanford 94305, California, United States;* orcid.org/0000-0002-7591-1496

Kathryn Langenfeld − *Department of Civil and Environmental Engineering, University of Michigan, Ann Arbor 48109, Michigan, United States*

Complete contact information is available at: https://pubs.acs.org/10.1021/acs.est.0c06191

Notes

The authors declare no competing financial interest.

◆K.E.G. and S.K.L. contributed equally to this work.

■ ACKNOWLEDGMENTS

This work was partially supported by NSF RAPID (CBET-2023057) grant to K.R.W. and A.B.B. and a Shimizu Visiting Professorship for K.R.W, and anonymous funding from a private family foundation. We thank B. Pinsky and M. Sahoo in Stanford Clinical Virology as well as an anonymous patient for providing our positive control SARS-CoV-2 RNA, and S. Spencer at USDA for providing the BCoV vaccine. N.S.-A. was funded by a Stanford Graduate Fellowship. We acknowledge San Mateo County Health for providing the case count data for the portion of the POTW A sewershed located in San Mateo County and POTW staff for providing samples. We acknowledge the County of Santa Clara Public Health Department, and Linlin Li for assisting with the case data. This study was performed on the ancestral and unceded lands of the Muwekma Ohlone people. We pay our respects to them and their Elders, past and present, and are grateful for the opportunity to live and work there.

■ REFERENCES

(1) Zuccato, E.; Chiabrando, C.; Castiglioni, S.; Bagnati, R.; Fanelli, R. Estimating Community Drug Abuse by Wastewater Analysis. *Environ. Health Perspect.* **2008**, *116*, 1027−1032.

(2) Gushgari, A. J.; Venkatesan, A. K.; Chen, J.; Steele, J. C.; Halden, R. U. Long-Term Tracking of Opioid Consumption in Two United States Cities Using Wastewater-Based Epidemiology Approach. *Water Res.* **2019**, *161*, 171−180.

(3) Manor, Y.; Handsher, R.; Halmut, T.; Neuman, M.; Bobrov, A.; Rudich, H.; Vonsover, A.; Shulman, L.; Kew, O.; Mendelson, E. Detection of Poliovirus Circulation by Environmental Surveillance in the Absence of Clinical Cases in Israel and the Palestinian Authority. *J. Clin. Microbiol.* **1999**, *37*, 1670.

(4) Brouwer, A. F.; Eisenberg, J. N. S.; Pomeroy, C. D.; Shulman, L. M.; Hindiyeh, M.; Manor, Y.; Grotto, I.; Koopman, J. S.; Eisenberg, M. C. Epidemiology of the Silent Polio Outbreak in Rahat, Israel, Based on Modeling of Environmental Surveillance Data. *Proc. Natl. Acad. Sci. U. S. A.* **2018**, *115*, E10625.

(5) McCall, C.; Wu, H.; Miyani, B.; Xagoraraki, I. Identification of Multiple Potential Viral Diseases in a Large Urban Center Using Wastewater Surveillance. *Water Res.* **2020**, *184*, 116160.

(6) Bisseux, M.; Colombet, J.; Mirand, A.; Roque-Afonso, A.-M.; Abravanel, F.; Izopet, J.; Archimbaud, C.; Peigue-Lafeuille, H.; Debroas, D.; Bailly, J.-L.; Henquell, C. Monitoring Human Enteric Viruses in Wastewater and Relevance to Infections Encountered in the Clinical Setting: A One-Year Experiment in Central France, 2014 to 2015. *Euro Surveill* **2018**, *23*, 17−00237.

(7) Diemert, S.; Yan, T. Clinically Unreported Salmonellosis Outbreak Detected via Comparative Genomic Analysis of Municipal Wastewater *Salmonella* Isolates. *Appl. Environ. Microbiol.* **2019**, *85*, e00139−e00119.

(8) Diemert, S.; Yan, T. Municipal Wastewater Surveillance Revealed a High Community Disease Burden of a Rarely Reported and Possibly Subclinical Salmonella Enterica Serovar Derby Strain. *Appl. Environ. Microbiol.* **2020**, *86*, e00814−e00820.

(9) Gupta, S.; Parker, J.; Smits, S.; Underwood, J.; Dolwani, S. Persistent Viral Shedding of SARS-CoV-2 in Faeces − a Rapid Review. *Colorectal Disease* **2020**, *22*, 611−620.

(10) Wu, Y.; Guo, C.; Tang, L.; Hong, Z.; Zhou, J.; Dong, X.; Yin, H.; Xiao, Q.; Tang, Y.; Qu, X.; Kuang, L.; Fang, X.; Mishra, N.; Lu, J.; Shan, H.; Jiang, G.; Huang, X. Prolonged Presence of SARS-CoV-2 Viral RNA in Faecal Samples. *Lancet Gastroenterol. Hepatol.* **2020**, *5*, 434−435.

(11) Pan, Y.; Zhang, D.; Yang, P.; Poon, L. L. M.; Wang, Q. Viral Load of SARS-CoV-2 in Clinical Samples. *Lancet Infect. Dis.* **2020**, *20*, 411−412.

(12) Harris, J. E. Overcoming Reporting Delays Is Critical to Timely Epidemic Monitoring: The Case of COVID-19 in New York City. *medRxiv* **2020**, DOI: 10.1101/2020.08.02.20159418.

(13) Arons, M. M.; Hatfield, K. M.; Reddy, S. C.; Kimball, A.; James, A.; Jacobs, J. R.; Taylor, J.; Spicer, K.; Bardossy, A. C.; Oakley, L. P.; Tanwar, S.; Dyal, J. W.; Harney, J.; Chisty, Z.; Bell, J. M.; Methner, M.; Paul, P.; Carlson, C. M.; McLaughlin, H. P.; Thornburg, N.; Tong, S.; Tamin, A.; Tao, Y.; Uehara, A.; Harcourt, J.; Clark, S.; Brostrom-Smith, C.; Page, L. C.; Kay, M.; Lewis, J.; Montgomery, P.; Stone, N. D.; Clark, T. A.; Honein, M. A.; Duchin, J. S.; Jernigan, J. A. Presymptomatic SARS-CoV-2 Infections and Transmission in a Skilled Nursing Facility. *N Engl J Med* **2020**, *382*, 2081−2090.

(14) Li, R.; Pei, S.; Chen, B.; Song, Y.; Zhang, T.; Yang, W.; Shaman, J. Substantial Undocumented Infection Facilitates the Rapid Dissemination of Novel Coronavirus (SARS-CoV-2). *Science* **2020**, *368*, 489.

(15) United States Center for Disease Control. *National Wastewater Surveillance System (NWSS)* https://www.cdc.gov/coronavirus/2019-ncov/cases-updates/wastewater-surveillance.html (accessed Aug 24, 2020).

(16) Gonzalez, R.; Curtis, K.; Bivins, A.; Bibby, K.; Weir, M. H.; Yetka, K.; Thompson, H.; Keeling, D.; Mitchell, J.; Gonzalez, D.

COVID-19 Surveillance in Southeastern Virginia Using Wastewater-Based Epidemiology. *Water Res.* **2020**, *186*, 116296.
(17) Medema, G.; Heijnen, L.; Elsinga, G.; Italiaander, R.; Brouwer, A. Presence of SARS-Coronavirus-2 RNA in Sewage and Correlation with Reported COVID-19 Prevalence in the Early Stage of the Epidemic in The Netherlands. *Environ. Sci. Technol. Lett.* **2020**, *7*, 511−516.
(18) Ahmed, W.; Angel, N.; Edson, J.; Bibby, K.; Bivins, A.; O'Brien, J. W.; Choi, P. M.; Kitajima, M.; Simpson, S. L.; Li, J.; Tscharke, B.; Verhagen, R.; Smith, W. J. M.; Zaugg, J.; Dierens, L.; Hugenholtz, P.; Thomas, K. V.; Mueller, J. F. First Confirmed Detection of SARS-CoV-2 in Untreated Wastewater in Australia: A Proof of Concept for the Wastewater Surveillance of COVID-19 in the Community. *Sci. Total Environ.* **2020**, *728*, 138764.
(19) Wu, F.; Zhang, J.; Xiao, A.; Gu, X.; Lee, W. L.; Armas, F.; Kauffman, K.; Hanage, W.; Matus, M.; Ghaeli, N.; Endo, N.; Duvallet, C.; Poyet, M.; Moniz, K.; Washburne, A. D.; Erickson, T. B.; Chai, P. R.; Thompson, J.; Alm, E. J. SARS-CoV-2 Titers in Wastewater Are Higher than Expected from Clinically Confirmed Cases. *mSystems* **2020**, *5*, e00614−e00620.
(20) Ahmed, W.; Bertsch, P. M.; Bivins, A.; Bibby, K.; Farkas, K.; Gathercole, A.; Haramoto, E.; Gyawali, P.; Korajkic, A.; McMinn, B. R.; Mueller, J. F.; Simpson, S. L.; Smith, W. J. M.; Symonds, E. M.; Thomas, K. V.; Verhagen, R.; Kitajima, M. Comparison of Virus Concentration Methods for the RT-QPCR-Based Recovery of Murine Hepatitis Virus, a Surrogate for SARS-CoV-2 from Untreated Wastewater. *Sci. Total Environ.* **2020**, *739*, 139960.
(21) Ye, Y.; Ellenberg, R. M.; Graham, K. E.; Wigginton, K. R. Survivability, Partitioning, and Recovery of Enveloped Viruses in Untreated Municipal Wastewater. *Environ. Sci. Technol.* **2016**, *50*, 5077−5085.
(22) Peccia, J.; Zulli, A.; Brackney, D. E.; Grubaugh, N. D.; Kaplan, E. H.; Casanovas-Massana, A.; Ko, A. I.; Malik, A. A.; Wang, D.; Wang, M.; Warren, J. L.; Weinberger, D. M.; Omer, S. B. Measurement of SARS-CoV-2 RNA in wastewater tracks community infection dynamics. *Nat. Biotechnol.* **2020**, *38*, 1164−1167.
(23) Bibby, K.; Viau, E.; Peccia, J. Viral Metagenome Analysis to Guide Human Pathogen Monitoring in Environmental Samples. *Lett. Appl. Microbiol.* **2011**, *52*, 386−392.
(24) Loeb, S.; Graham, K.; Wolfe, M.; Wigginton, K.; Boehm, A. Extraction of RNA from Wastewater Primary Solids Using a Direct Extraction Method for Downstream SARS-CoV-2 RNA Quantification. *protocols.io* **2020**, DOI: 10.17504/protocols.io.bi6skhee.
(25) Bustin, S. A.; Benes, V.; Garson, J. A.; Hellemans, J.; Huggett, J.; Kubista, M.; Mueller, R.; Nolan, T.; Pfaffl, M. W.; Shipley, G. L.; Vandesompele, J.; Wittwer, C. T. The MIQE Guidelines: Minimum Information for Publication of Quantitive Real-Time PCR Experiments. *Clin. Chem.* **2009**, *55*, 611−622.
(26) Loeb, S.; Graham, K.; Catoe, D.; Wolfe, M.; Boehm, A.; Wigginton, K. One-Step RT-DdPCR for Detection of SARS-CoV-2, Bovine Coronavirus, and PMMoV RNA in RNA Derived from Wastewater or Primary Settled Solids. *protocols.io* **2020**, DOI: 10.17504/protocols.io.bi6vkhe6.
(27) The dMIQE Group; Huggett, J. F. The Digital MIQE Guidelines Update: Minimum Information for Publication of Quantitative Digital PCR Experiments for 2020. *Clin. Chem.* **2020**, *66*, 1012−1029.
(28) Dickey, D. A.; Fuller, W. A. Distribution of the Estimators for Autoregressive Time Series With a Unit Root. *J. Am. Stat. Assoc.* **1979**, *74*, 427−431.
(29) Loeb, S.; Graham, K.; Wolfe, M.; Catoe, D.; Sinnott-Armstrong, N.; Kim, S.; Yamahara, K. M.; Sassoubre, L. M.; Mendoza, L.; Roldan-Hernandez, L.; Wigginton, K. R.; Boehm, A. B. SARS-CoV-2 RNA in settled solids from a large urban wastewater treatment plant https://purl.stanford.edu/ct379mv1537.
(30) Yin, Z.; Voice, T. C.; Tarabara, V. V.; Xagoraraki, I. Sorption of Human Adenovirus to Wastewater Solids. *J. Environ. Eng.* **2018**, *144*, No. 06018008.
(31) Berg, G. Removal of Viruses from Sewage, Effluents, and Waters. I. A Review. *Bull. W. H. O.* **1973**, *49*, 451−460.
(32) Ward, R. L. Virus Survival During Sludge Treatment. In *Viruses and Wastewater Treatment*; Goddard, M., Butler, M., Eds.; Pergamon: 1981; pp. 65−77, DOI: 10.1016/B978-0-08-026401-1.50015-4.
(33) Chalapati Rao, V.; Metcalf, T. G.; Melnick, J. L. Removal of Indigenous Rotaviruses during Primary Settling and Activated-Sludge Treatment of Raw Sewage. *Water Res.* **1987**, *21*, 171−177.
(34) D'Aoust, P. M.; Mercier, E.; Montpetit, D.; Jia, J.-J.; Alexandrov, I.; Neault, N.; Baig, A. T.; Mayne, J.; Zhang, X.; Alain, T.; Langlois, M.-A.; Servos, M. R.; MacKenzie, M.; Figeys, D.; MacKenzie, A. E.; Graber, T. E.; Delatolla, R. Quantitative Analysis of SARS-CoV-2 RNA from Wastewater Solids in Communities with Low COVID-19 Incidence and Prevalence. *Water Res.* **2021**, *188*, 116560.
(35) Zwald, M. L.; Lin, W.; Cooksey, G. L. S.; Weiss, C.; Suarez, A.; Fischer, M.; Bonin, B. J.; Jain, S.; Langley, G. E.; Park, B. J.; Moulia, D.; Benedict, R.; Nguyen, N.; Han, G. Rapid Sentinel Surveillance for COVID-19 — Santa Clara County, California, March 2020. *Morb. Mortal. Wkly. Rep.* **2020**, *69*, 419−421.
(36) Xu, Y.; Li, X.; Zhu, B.; Liang, H.; Fang, C.; Gong, Y.; Guo, Q.; Sun, X.; Zhao, D.; Shen, J.; Zhang, H.; Liu, H.; Xia, H.; Tang, J.; Zhang, K.; Gong, S. Characteristics of Pediatric SARS-CoV-2 Infection and Potential Evidence for Persistent Fecal Viral Shedding. *Nat. Med.* **2020**, *26*, 502−505.
(37) Chen, C.; Gao, G.; Xu, Y.; Pu, L.; Wang, Q.; Wang, L.; Wang, W.; Song, Y.; Chen, M.; Wang, L.; Yu, F.; Yang, S.; Tang, Y.; Zhao, L.; Wang, H.; Wang, Y.; Zeng, H.; Zhang, F. SARS-CoV-2−Positive Sputum and Feces After Conversion of Pharyngeal Samples in Patients With COVID-19. *Ann. Intern. Med.* **2020**, *172*, 832−834.
(38) Wölfel, R.; Corman, V. M.; Guggemos, W.; Seilmaier, M.; Zange, S.; Müller, M. A.; Niemeyer, D.; Jones, T. C.; Vollmar, P.; Rothe, C.; Hoelscher, M.; Bleicker, T.; Brünink, S.; Schneider, J.; Ehmann, R.; Zwirglmaier, K.; Drosten, C.; Wendtner, C. Virological Assessment of Hospitalized Patients with COVID-2019. *Nature* **2020**, 465.
(39) Dingle, T. C.; Sedlak, R. H.; Cook, L.; Jerome, K. R. Tolerance of Droplet-Digital PCR vs Real-Time Quantitative PCR to Inhibitory Substances. *Clin. Chem.* **2013**, *59*, 1670−1672.
(40) Wang, D.; Yamahara, K. M.; Cao, Y.; Boehm, A. B. Absolute Quantification of Enterococcal 23S RRNA Gene Using Digital PCR. *Environ. Sci. Technol.* **2016**, *50*, 3399−3408.
(41) Schrader, C.; Schielke, A.; Ellerbroek, L.; Johne, R. PCR Inhibitors − Occurrence, Properties and Removal. *Journal of Applied Microbiology* **2012**, *113*, 1014−1026.
(42) Kreader, C. A. Relief of Amplification Inhibition in PCR with Bovine Serum Albumin or T4 Gene 32 Protein. *Appl. Environ. Microbiol.* **1996**, *62*, 1102.
(43) Randazzo, W.; Truchado, P.; Cuevas-Ferrando, E.; Simón, P.; Allende, A.; Sánchez, G. SARS-CoV-2 RNA in Wastewater Anticipated COVID-19 Occurrence in a Low Prevalence Area. *Water Res.* **2020**, *181*, 115942.
(44) Mlejnkova, H.; Sovova, K.; Vasickova, P.; Ocenaskova, V.; Jasikova, L.; Juranova, E. Preliminary Study of Sars-Cov-2 Occurrence in Wastewater in the Czech Republic. *Int. J. Environ. Res. Public Health* **2020**, *17* (), DOI: 10.3390/ijerph17155508.
(45) Viau, E. J.; Lee, D.; Boehm, A. B. Swimmer Risk of Gastrointestinal Illness from Exposure to Tropical Coastal Waters Impacted by Terrestrial Dry-Weather Runoff. *Environ. Sci. Technol.* **2011**, *45*, 7158−7165.
(46) Deboosere, N.; Horm, S. V.; Delobel, A.; Gachet, J.; Buchy, P.; Vialette, M. Viral Elution and Concentration Method for Detection of Influenza A Viruses in Mud by Real-Time RT-PCR. *J. Virol. Methods* **2012**, *179*, 148−153.
(47) van Nuijs, A. L. N.; Mougel, J.-F.; Tarcomnicu, I.; Bervoets, L.; Blust, R.; Jorens, P. G.; Neels, H.; Covaci, A. Sewage Epidemiology — A Real-Time Approach to Estimate the Consumption of Illicit Drugs in Brussels, Belgium. *Environ. Int.* **2011**, *37*, 612−621.

(48) Castiglioni, S.; Bijlsma, L.; Covaci, A.; Emke, E.; Hernández, F.; Reid, M.; Ort, C.; Thomas, K. V.; van Nuijs, A. L. N.; de Voogt, P.; Zuccato, E. Evaluation of Uncertainties Associated with the Determination of Community Drug Use through the Measurement of Sewage Drug Biomarkers. *Environ. Sci. Technol.* **2013**, *47*, 1452−1460.
(49) Been, F.; Rossi, L.; Ort, C.; Rudaz, S.; Delémont, O.; Esseiva, P. Population Normalization with Ammonium in Wastewater-Based Epidemiology: Application to Illicit Drug Monitoring. *Environ. Sci. Technol.* **2014**, *48*, 8162−8169.
(50) Symonds, E. M.; Nguyen, K. H.; Harwood, V. J.; Breitbart, M. Pepper Mild Mottle Virus: A Plant Pathogen with a Greater Purpose in (Waste)Water Treatment Development and Public Health Management. *Water Res.* **2018**, *144*, 1−12.
(51) Ahmed, W.; Bertsch, P. M.; Bibby, K.; Haramoto, E.; Hewitt, J.; Huygens, F.; Gyawali, P.; Korajkic, A.; Riddell, S.; Sherchan, S. P.; Simpson, S. L.; Sirikanchana, K.; Symonds, E. M.; Verhagen, R.; Vasan, S. S.; Kitajima, M.; Bivins, A. Decay of SARS-CoV-2 and Surrogate Murine Hepatitis Virus RNA in Untreated Wastewater to Inform Application in Wastewater-Based Epidemiology. *Environ. Res.* **2020**, *191*, 110092.
(52) Curtis, K.; Keeling, D.; Yetka, K.; Larson, A.; Gonzalez, R. Wastewater SARS-CoV-2 Concentration and Loading Variability from Grab and 24-Hour Composite Samples. *medRxiv* **2020**, DOI: 10.1101/2020.07.10.20150607.

https://dx.doi.org/10.1021/acs.est.0c06191
Environ. Sci. Technol. 2021, 55, 488−498